Journal of Alloys and Compounds 505 (2010) 1–5

Contents lists available at ScienceDirect

Journal of Alloys and Compounds

journal homepage: www.elsevier.com/locate/jallcom

A series of $BaAl_{2-x}Si_xH_{2-x}$ ($0.4 < x < 1.6$) hydrides with compositions and structures in between $BaSi_2$ and $BaAl_2H_2$

D. Moser[a,c], U. Häussermann[b], T. Utsumi[c], T. Björling[c], D. Noréus[c,*]

[a] Materials & Physics Research Centre, Salford University, M5 4WT Greater Manchester, UK
[b] Department of Chemistry and Biochemistry, Arizona State University, United States
[c] Department of Materials and Environmental Chemistry, Stockholm University, SE-10691 Stockholm, Sweden

ARTICLE INFO

Article history:
Received 24 March 2010
Received in revised form 10 May 2010
Accepted 13 May 2010
Available online 27 May 2010

Keywords:
Aluminium hydrides
Band gap
X-ray powder diffraction

ABSTRACT

By substituting Si^- with $(Al–H)^-$ in trigonal $BaSi_2$, a series of hydrides has been synthesized with compositions $BaAl_{2-x}Si_xH_{2-x}$ ($0.4 < x < 1.6$). DFT calculations show that the end compositions $BaSi_2$ and $BaAl_2H_2$ are conductors whereas the intermediate BaAlSiH is a semiconductor. The cell parameters for the trigonal cell vary linearly as a function of the $Si^-/(Al–H)^-$ substitution in this MgB_2 related structure type, opening up the possibility of continuously tunable electric properties.

1. Introduction

$BaSi_2$ is an interesting compound; three structures with distinct properties have so far been observed: an orthorhombic phase which is stable at ambient conditions and two metastable high pressure phases, a cubic and a trigonal [1–4]. Both high pressure phases can be retained at ambient conditions, if the samples are rapidly quenched from the high pressure synthesis. The cubic and trigonal phases are obtained by subjecting the orthorhombic phase to a pressure of 4 GPa at 600–800 or 1000 °C, respectively [2,3]. Trigonal $BaSi_2$ is an electrical conductor and has been reported to be a superconductor with an critical temperature of 6.8 K [5,6]. A similar trigonal $CaSi_2$ phase has been reported with an unusual high T_c of 14 K [7]. Cubic and orthorhombic $BaSi_2$ phases are semiconductors [8]. The latter, with a bandgap of 1.3 eV, has been considered to be a good candidate for solar cell materials [9]. This paper will solely focus on modifications in the trigonal system. The structure of BaAlSiH is closely related to trigonal $BaSi_2$, but the substitution modifies the electric properties. The density of states (DOS) of BaAlSiH showed a narrow band gap of 0.8 eV [10]. CaAlSiH and SrAlSiH are also semiconductors [10,11]. BaAlSiH can be obtained by direct hydrogenation of the precursor BaAlSi. In BaAlSiH, every second Si^- ion in $BaSi_2$ is substituted with an isoelectronic $[AlH]^-$ entity. The BaAlSi, precursor material of BaAlSiH, itself is interesting. Recently, Yamanaka et al. reported a superconductor transition with $T_c = 2.8$ K in the BaAlSi system [12]; they revealed that Al/Si ratio in BaAlSi is changeable according to $BaAl_{2-x}Si_x$ ($1 < x < 1.5$). However, superconductivity was only observed for $x > 1$. The corresponding CaAlSi and SrAlSi are also superconductors with T_cs at 7.8 and 5.1 K, respectively [13]. In addition to the metal to non-metal transition, hydrogenation introduces a change in the vibrational properties by removing the soft mode related to superconducting properties. Thus, hydrogenation is probably an unfavourable way to improve the superconducting properties of these systems [11].

The aim of this work is to investigate the hydrogenation of the different $BaAl_{2-x}Si_x$ alloys in the trigonal system. The limiting compositions are $BaAl_2H_2$ and $BaSi_2$ ($x = 0$ and 2 in $BaAl_{2-x}Si_xH_{2-x}$). $BaAl_2$, and the corresponding hydride $BaAl_2H_2$, have not been observed experimentally, as all the synthesis attempts have proven so far unsuccessful, their properties were calculated by means of density functional theory. Attempts to extend the experimental investigation to the Ca- and Sr-analogues were not satisfactory due to larger amounts of impurity phases. This was recently confirmed by Zhu et al. who tried to synthesize and hydride a corresponding $SrAl_{2-x}Si_xH_{2-x}$ series in between $SrAl_2$ and SrAlSi [14]. They found that hydrogenation lead to various mixtures of SrAlSi, SrAlSiH, $SrAl_2$, SrH_2 and $SrAl_4$ phases. The Ba-system seemed to be more forgiving when manipulating the composition. In the Ba-system we thus synthesized and characterized a series of hydrides according to $BaAl_{2-x}Si_xH_{2-x}$ ($0 < x < 2$). Fig. 1 shows a hypothetical calculated $BaAl_2H_2$ ($x = 0$), BaAlSiH ($x = 1$) and the trigonal structure of $BaSi_2$ ($x = 2$); they are structurally related having a trigonal network of an $[Al_{2-x}Si_xH_{2-x}]^-$ anion sandwiched by Ba^{2+} ions. A simple electron count would suggest straight forward sp^3 hybridization for

* Corresponding author.
E-mail address: dag@struc.su.se (D. Noréus).

0925-8388/$ – see front matter © 2010 Elsevier B.V. All rights reserved.
doi:10.1016/j.jallcom.2010.05.065

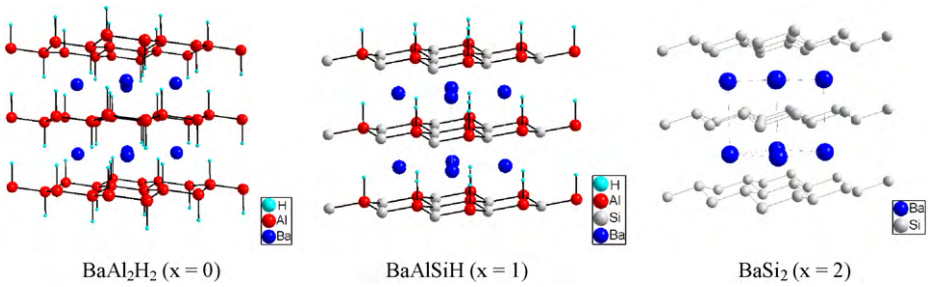

Fig. 1. Structures of $BaAl_{2-x}Si_xH_{2-x}$ (x = 0, 1 and 2).

the anion. Non-metallic BaAlSiH and electric conducting $BaSi_2$ and $BaAl_2H_2$ indicate a more complex situation as the $(AlH)^-$ unit is substituted by an isoelectronic Si^- (Si-lone pair), when going from $BaAl_2H_2$ to $BaSi_2$. In this paper we report cell parameters for the precursor $BaAl_{2-x}Si_x$ ($0.4 < x < 1.6$) as well as for the corresponding hydrides. This type of systems could have tunable electric properties correlated with the above described substitution.

2. Experimental details

2.1. Synthesis

Sample handling was carried out under argon atmosphere. Commercially pure Si powder, Al powder, and Ba ingot were obtained from MERCK, Alfa Aesar and Aldrich, respectively. The $BaAl_{2-x}Si_x$ ($0.4 < x < 1.6$) alloys were synthesized by melting stoichiometric ratios of the elements in a MAM-1 (Edmund Buhler) arc melting furnace. The heating current was 15 A and the ingot cup was water cooled. All samples were analyzed by means of X-ray powder diffraction as described below. Some samples exhibited diffraction patterns with rather broad peaks which were attributed to poor crystallinity especially in the case of aluminium rich samples. In order to improve crystallization, Al rich samples were annealed with a heat treatment at 500 °C for 2 days, whereby the width of the diffraction peaks indeed decreased. The $BaAl_{2-x}Si_x$ ($0.4 < x < 1.6$) samples were crushed into powders and placed into corundum tubes inserted into a sealed stainless steel autoclave, where they reacted with hydrogen. The reaction temperature was recorded with a stainless steel encapsulated thermocouple inserted directly into the powder. The hydrogenation conditions are resumed in Table 1.

2.2. X-ray powder diffraction

All reactants and products obtained were investigated by means of powder X-ray diffraction, using a Guinier–Hägg focusing camera of diameter 40 mm, with monochromated Cu $K_{\alpha 1}$ radiation (λ = 1.5405980 Å). Silicon was used as an internal standard. The films were measured in an LS 18 film scanner [15]. The program SCANPI [16] was used to determine d-values and intensities in the films. The Program TREOR [17] and PIRUM [18] were used for indexing and refining unit cell parameters.

2.3. Diffuse reflectance measurements

The band gap of a finely ground BaAlSiH sample was evaluated by recording the optical diffuse reflectance spectra in the 3200–10500 cm^{-1} region with a Bruker Equinox 55 FT-IR spectrometer equipped with a diffuse reflectance accessory (Harrick). The absorption data were extracted from the reflectance data by using the Kubelka–Munk function; $F(R) = (1-R)^2/2R$. This allows the optical absorbance of a sample to be approximated from its reflectance, R [19]. A Tauc plot can be obtained from the measured data if $(F(R) \times h\nu)^n$ is plotted vs $h\nu$. For a direct band gap semiconductor, a plot with $n = 1/2$ will show a linear Tauc region just above the optical-absorption edge. An indirect semiconductor would show a Tauc region in an $n = 2$ plot. It should be kept in mind, however, that small band gaps are difficult to measure correctly. Errors in the fit procedure as well as uncertainties in hydrogen content and possible topological disorders add to these difficulties.

2.4. Computational details

Total-energy calculations for $BaAl_2H_2$, BaAlSiH and $BaSi_2$ were performed in the framework of the frozen core all-electron projected augmented wave (PAW) method [20], as implemented in the program VASP [21]. The energy cut-off was set to 500 eV. Exchange and correlation effects were treated by the generalized gradient approximation (GGA), usually referred to as PW91 [22]. The integration over the Brillouin zone was done on special gamma centred k-point mesh determined according to the Monkhorst–Pack scheme [23]. Total energies were converted to at least 1 meV/atom. Structural parameters were relaxed until forces had converged to less than 0.01 eV/Å. The equilibrium structure of $SrAl_2H_2$ [24] was used as starting configuration for $BaAl_2H_2$. The partial density of states are depicted in Fig. 5a–c and the total density of states in Fig. 5d.

3. Results and discussion

In the $BaAl_{2-x}Si_x$ ($0.4 < x < 1.6$) series, only BaAlSi (with x = 1) showed a single phase in the XRD pattern. $BaAl_{2-x}Si_x$ ($0.4 < x < 1.6$) samples, deviating from x = 1, exhibited secondary phases in the diffraction patterns, which were not eliminated by heat treatments. For x-values above 1, small peaks of $BaAl_2Si_2O_8$ [25], $BaSi_2$ (orthorhombic) [1] and also some unknown impurity peaks were observed. For x-values below 1, some other unidentified peaks were observed. The amount of the impurity phases was, however, not enough to allow identification. As x increasingly deviates from 1, the intensity of the impurity peaks increases; this introduces a small systematic error in the targeted $BaAl_{2-x}Si_x$ compositions, especially at higher deviation from x = 1. Nevertheless, we estimated the deviations to be small and not significantly affecting the general conclusions.

The $BaAl_{2-x}Si_x$ crystallizes with hexagonal symmetry in space group $P6/mmm$ (1 9 1) (cf. Fig. 2) [26] and its structure consists of hexagonal $[Al_{2-x}Si_x]^{2-}$ layers, which are stacked on top of each other. The Ba^{2+} ions are sandwiched between these layers.

The detailed ordering of Al/Si in $BaAl_{2-x}Si_x$ is not clear, as Al and Si are neighbours in the periodic table making them difficult to distinguish by XRD. It was originally assumed that Si and Al atoms are more or less randomly distributed in the hexagonal network, but research done by Akimitsu et al. [27] on CaAlSi indicated that the atoms in the poly anionic network are ordered and therefore the symmetry description of CaAlSi is better described by space group $P\bar{6}m2$ instead of $P6/mmm$.

Fig. 3 and Table 2 show the cell parameter and cell volume change of $BaAl_{2-x}Si_x$ ($0.4 < x < 1.6$). The a-axis and cell volume decrease linearly with increasing x-value. This is reasonable as

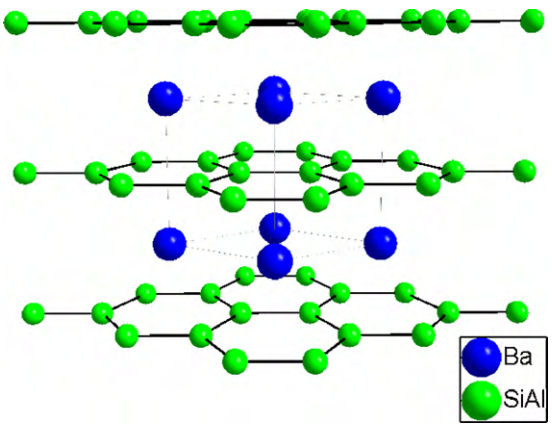

Fig. 2. Structure of $BaAl_{2-x}Si_x$ (space group 191).

Table 1
Hydrogenation of the alloys at 70 bar H_2.

Composition	Temp [°C]	Time [h]	XRD phase analysis
$BaAl_{1.6}Si_{0.4}$	300	48	Formation of an assumed $BaAl_{1.6}Si_{0.4}H_{1.6}$. Unknown phases were also observed.
	700	48	Formation of BaAlSiH instead $BaAl_{0.4}Si_{1.6}H_{0.4}$. Unknown phases were also observed.
$BaAl_{1.4}Si_{0.6}$	300	48	Formation of an assumed $BaAl_{1.4}Si_{0.6}H_{1.4}$. Additionally, small peaks of unknown phases are observed.
	550	3	Formation of an assumed $BaAl_{1.4}Si_{0.6}H_{1.4}$. Additionally, BaAlSiH and unknown phases were also observed.
	600	3	Formation of an assumed $BaAl_{1.4}Si_{0.6}H_{1.4}$. Additionally, unknown phases are also observed as a second phase.
$BaAl_{0.6}Si_{1.4}$	300	48	No hydride was formed.
	550	3	Formation of an assumed $BaAl_{0.6}Si_{1.4}H_{0.6}$, but additionally $BaSi_2$ and unknown phases were also observed.
	600	12	Formation of a phase close to $BaAl_{0.6}Si_{1.4}H_{0.6}$. Additionally $BaSi_2$ and unknown phases were also observed.
	700	48	Formation of BaAlSiH instead of $BaAl_{0.6}Si_{1.4}H_{0.6}$. Additionally $BaSi_2$ and unknown phases are also observed.
$BaAl_{0.4}Si_{1.6}$	300	48	Formation of an assumed $BaAl_{0.4}Si_{1.6}H_{0.4}$. Additionally, small peaks of $BaSi_2$ and unknown phases were observed.
	500	48	Formation of a phase closes to $BaAl_{0.6}Si_{1.4}H_{0.6}$ instead $BaAl_{0.4}Al_{1.6}H_{0.4}$. Strong peaks of $BaSi_2$, BaSi and unknown phases were also observed.
	700	48	Formation of BaAlSiH instead of $BaAl_{0.4}Si_{1.6}H_{0.4}$. Strong peaks of $BaSi_2$, BaSi and unknown phases were also observed.

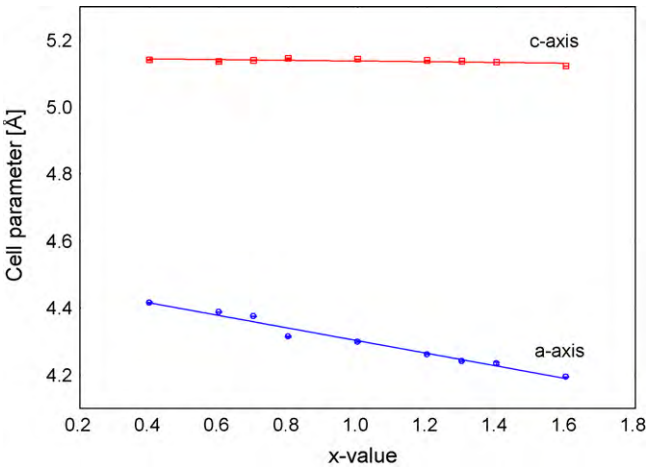

Fig. 3. Cell parameters of $BaAl_{2-x}Si_x$ as a function of *x*.

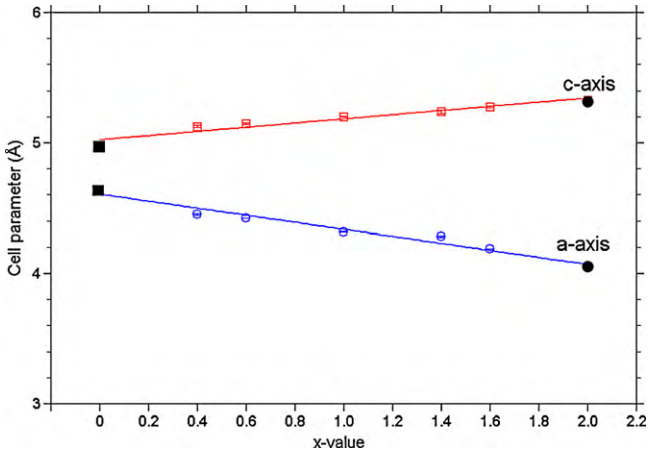

Fig. 4. Cell parameters of $BaAl_{2-x}Si_xH_{2-x}$ (computationally obtained $BaAl_2H_2$, ■; $BaSi_2$, ● [2]).

larger Al atoms are replaced by smaller Si atoms. The *c*-axis is relatively independent of *x*. These trends were also reported by Yamanaka et al. [12]. For the BaAlSi ($x = 1$) phase, the cell parameter could be indexed with $a = 4.2989(6)$ Å and $c = 5.1437(7)$ Å in good agreement with the previously reported BaAlSi, $a = 4.290$ Å and $c = 5.140$ Å [13].

The corresponding hydrides $BaAl_{2-x}Si_xH_{2-x}$ ($0.4 < x < 1.6$) were synthesized by direct hydrogenation of the $BaAl_{2-x}Si_x$ alloys, as

Table 2
Cell parameters of $BaAl_{2-x}Si_x$ and $BaAl_{2-x}Si_xH_{2-x}$ for each *x*-value.

Composition	*a*-Axis [Å]	*c*-Axis [Å]	*V* [Å^3]
$BaAl_{1.6}Si_{0.4}$	4.416(2)	5.141(2)	86.82(7)
$BaAl_{1.4}Si_{0.6}$	4.3884(9)	5.137(2)	85.67(4)
$BaAl_{1.3}Si_{0.7}$	4.3757(8)	5.141(1)	85.25(3)
$BaAl_{1.2}Si_{0.8}$	4.315(2)	5.146(2)	82.98(6)
BaAlSi	4.2989(6)	5.1437(7)	82.32(2)
$BaAl_{0.8}Si_{1.2}$	4.2610(3)	5.1403(4)	80.82(1)
$BaAl_{0.7}Si_{1.3}$	4.2414(5)	5.1381(8)	80.08(2)
$BaAl_{0.6}Si_{1.4}$	4.2342(4)	5.1345(6)	79.72(1)
$BaAl_{0.4}Si_{1.6}$	4.1948(3)	5.1230(6)	78.07(1)
$BaAl_2H_2$ (calculated)	4.6524	4.9768	93.29
$BaAl_{1.6}Si_{0.4}H_{1.6}$	4.451(3)	5.125(4)	87.9(1)
$BaAl_{1.4}Si_{0.6}H_{1.4}$	4.4205(7)	5.145(2)	87.07(4)
BaAlSiH	4.3145(5)	5.2049(7)	83.91(2)
$BaAl_{0.6}Si_{1.4}H$	4.283(3)	5.238(5)	83.2(1)
$BaAl_{0.4}Si_{1.6}H$	4.187(1)	5.275(2)	80.09(4)
$BaSi_2$ [2]	4.047(3)	5.330(5)	75.6(1)

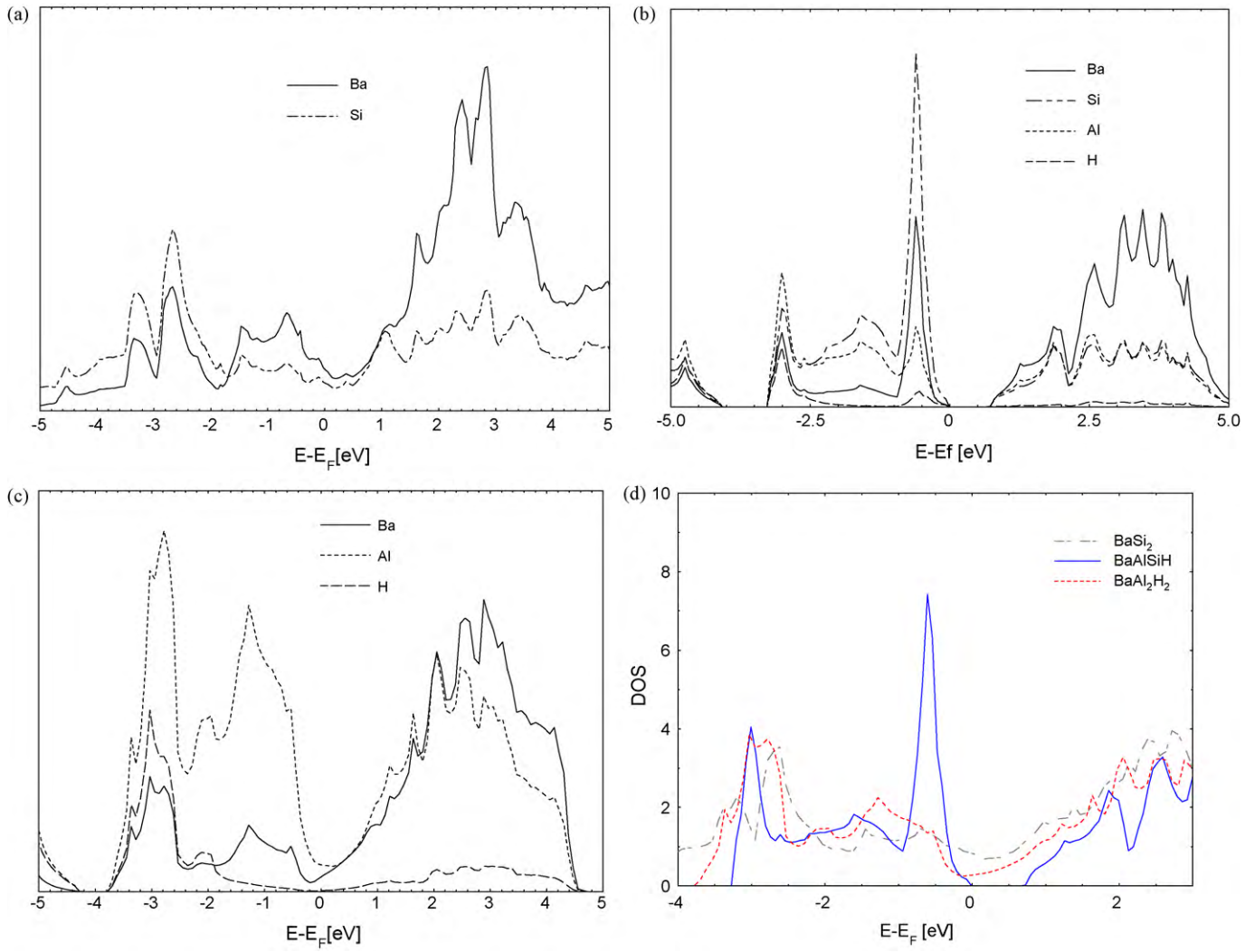

Fig. 5. Partial density of states of (a) $BaSi_2$, (b) BaAlSiH, (c) $BaAl_2H_2$ and (d) DOS of $BaAl_{2-x}Si_xH_{2-x}$ (x = 0, 1 and 2).

described in Table 1, where also the results from subsequent XRD phase analysis are given. During hydrogenation, the colour changed from metallic silver to dark gray. Careful control of the hydrogenation conditions was necessary; to hydrogenate BaAlSi (x = 1), 600 °C temperature and 70 bar of hydrogen pressure was required. On the other hand, hydrogenation of $BaAl_{1.6}Si_{0.4}$ (x = 0.4) and $BaAl_{0.4}Si_{1.6}$ (x = 1.6) starts at a lower temperature, 300 °C, at 70 bar of hydrogen pressures. Interestingly, at higher temperatures, aluminium rich $BaAl_{2-x}Si_xH_{2-x}$ ($0 < x < 1$) tend to decompose into a composition close to BaAlSiH (x = 1) and $BaAl_4$ [28] together to other impurity phases. Furthermore, at higher temperature, also silicon rich $BaAl_{2-x}Si_xH_{2-x}$ ($1 < x < 2$) tend to decompose to composition close to BaAlSiH (x = 1) and $BaSi_2$ [1] and other impurity phases. This indicates that BaAlSiH (x = close to 1) is an especially stable phase in the system. A similar situation was also observed for $SrAl_2H_2$ and SrAlSiH [11]. The hydrogen release in $SrAl_2H_2$ starts upon heating at 300 °C, whereas SrAlSiH is stable up to 600 °C. Higher temperatures are also needed for the hydrogenation of SrAlSi (600 °C and 50 bar) compared to a much lower value for $SrAl_2$ (190 °C) [24]. The 1:1:1 composition is thus especially stable both as an alloy and a hydride.

The obtained cell parameters are shown in Fig. 4 and Table 2. The unit cell parameters fit well between those of the computationally obtained $BaAl_2H_2$ (x = 0) and the previously reported $BaSi_2$ (x = 2) [1,2]. When going from $BaAl_2H_2$ to $BaSi_2$ by substituting $(Al–H)^-$ entities with $(Si)^-$-lone pairs, the *ab*-plane shrinks in good agreement with the difference in covalent radius between Al and Si. The decrease of the *a*-axis in the hydrides is almost identical to that in the alloys, indicating that the direct covalent bonding between Al/Si or Si/Si in the network is not much affected by the substitution. On the other hand the *c*-axis expands as the $(Al–H)^-$ entities are substituted by an increasing number of repulsive $(Si)^-$-lone pairs indicating that more space is required than for $(Al–H)^-$ entities. Interestingly, the puckering angle in the Si/Al network is also increasing up to 111°, close to the ideal sp^3 angle, when reaching $BaSi_2$. The increase in *c*-axis is also followed by an increase in the Al–H bond distance. The computational obtained Al–H distance is 1.71 Å in $BaAl_2H_2$ but increases to 1.74 Å in BaAlSiH. The difference in the Al–H distance is slightly less than that in the Sr-system. In $SrAl_2H_2$ the Al–H bond is 1.706 Å, which increases to 1.77 Å in SrAlSiH.

It is interesting to compare the synthesis condition of $BaSi_2$ and $BaAl_{2-x}Si_xH_{2-x}$. Trigonal $BaSi_2$ requires a high isostatic pressure to be formed. However, by substituting Si^- with $[Al–H]^-$, a trigonal $BaAl_{0.4}Si_{1.6}H_{0.4}$, structurally close to $BaSi_2$, could be obtained at milder conditions, 300 °C and 70 bar of hydrogen pressure.

We also observed an interesting stability problem when hydrogenating the precursor $BaAl_{2-x}Si_x$ alloys with compositions different from a 1:1:1 stoichiometry. If aluminium rich $BaAl_{2-x}Si_x$ ($0 < x < 1$) or silicon rich $BaAl_{2-x}Si_x$ ($1 < x < 0$) are hydrogenated at

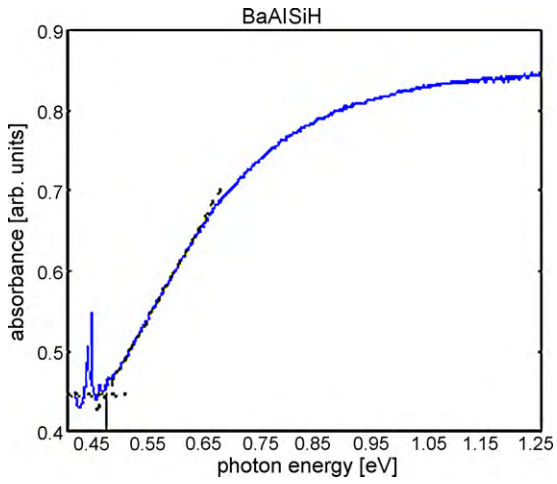

Fig. 6. Tauc plot of BaAlSiH. The square ($n = 2$) of the optical-absorption coefficient vs. the photon energy. The dotted line shows the Tauc extrapolation [19].

the lowest possible temperatures for the reaction, then a hydride with the same metal atom composition is obtained. However, if the temperature is increased, the hydride composition will start to move toward the stable 1:1:1 ratio. At this composition all the $[Al–H]^-$ and the silicon-lone pairs point out from separate sides of the network; this probably leads to a more relaxed structure and with the electrons being localized, a more simple description in terms of a sp^3 hybridization can be justified. Instead, as the composition deviates from the 1:1:1 ratio, either hydrogen or electron lone pairs appear mixed with increased overlap problems.

Density of states calculations (using DFT) suggests BaAlSiH to be a semiconductor with a narrow band gap of 0.71 eV in agreement with Ref. [11]. Trigonal $BaSi_2$ ($x = 2$) is reported to be an electric conductor [3] which could also be confirmed by our calculations above. The DOS calculation for $BaAl_2H_2$ indicates metallic conductivity. This is of great interest, in fact by substituting Si^- with $[AlH]^-$ in $BaAl_{2-x}Si_xH_{2-x}$, the electric property of $BaAl_{2-x}Si_xH_{2-x}$ can be changed. We expect that at some x-value between 1 and 2, a transformation from a semiconductor to a metallic conductor will occur and again at some x-value between 1 and 0, the transition will be reversed. In other word, the band gap will be tunable by substituting Si^- with $[AlH]^-$.

An indirect band gap of BaAlSiH was measured to be 0.5 eV in Fig. 6. This confirms a small band gap close to the calculated values between 0.7 and 0.8 eV. It should be kept in mind, however, that small band gaps are both difficult to calculate as well as to measure correctly. Attempts to measure band gaps for other hydrides in the system $BaAl_{2-x}Si_xH_{2-x}$ failed because of impurity phases present.

4. Conclusion

A series of hydrides with closely related structures ($BaAl_{2-x}Si_xH_{2-x}$) has been synthesized in between $BaSi_2$ and $BaAl_2H_2$, by gradual substitution of Si^- (a silicon-lone pairs) with isoelectric $[AlH]^-$ entities. The structure in this trigonal system can be described by a two dimensional network of interconnected $[Al_{2-x}Si_xH_{2-x}]^{2-}$ ions sandwiching Ba^{2-} ions. A simple electron count would suggest straight forward sp^3 hybridization in the network. Metallic $BaSi_2$ and $BaAl_2H_2$ encompassing semiconducting BaAlSiH indicate a more complex electron structure, at least at each end of the compositional chain. This opens up for interesting electric phenomena related to this tunable substitution. Hydrides, close to the 1:1:1 metal atom ratio as BaAlSiH, were more stable. At this composition all the $[Al–H]^-$ or silicon-lone pairs point away from separate sides of the network. As the composition deviates from the 1:1:1 ratio either H or electron lone pairs appear together on the same side with increasing overlap problems.

Acknowledgements

We would like to thank Scandinavia–Japan Sasakawa Foundation for support as well as the Swedish Energy Agency and the European Commission DG Research (contract SES6-2006-518271/NESSHY).

References

[1] H. Schäfer, K.H. Janzon, A. Weiss, Angew. Chem. Int. Ed. Engl. 2 (1963) 393.
[2] J. Evers, G. Oehlinger, A. Weiss, Angew. Chem. Int. Ed. Engl. 16 (1977) 659.
[3] J. Evers, G. Oehlinger, A. Weiss, Angew. Chem. Int. Ed. Engl. 17 (1978) 538.
[4] J. Evers, J. Solid State Chem. 32 (1980) 77.
[5] M. Imai, T. Hirano, J. Alloys Compd. 55 (1997) 132.
[6] M. Imai, K. Hirata, T. Hirano, Physica C 245 (1995) 12.
[7] M. Affronte, S. Sanfilippo, M. Nunez-Regueiro, O. Laborde, S. Lefloch, P. Bordet, M. Hanfland, D. Levi, A. Palenzona, G.L. Olcese, Physica B 284–288 (2000) 1117.
[8] M. Imai, T. Hirano, J. Alloys Compd. 224 (1995) 111.
[9] J. Evers, A. Weiss, Mater. Res. Bull. 9 (1974) 549.
[10] M.H. Lee, T. Björling, B.C. Hauback, T. Utsumi, D. Moser, D. Bull, D. Noréus, O.F. Sankey, U. Häussermann, Phys. Rev. B 78 (2008) 195209.
[11] T. Björling, D. Noréus, K. Jansson, M. Andersson, E. Lenova, M. Edén, U. Hålenius, U. Häussermann, Angew. Chem. Int. Ed. 44 (2005) 7269.
[12] S. Yamanaka, T. Otsuki, T. Ide, H. Fukuoka, R. Kumashiro, T. Rachi, K. Tanigaki, F. Guo, K. Kobayashi, Physica C 451 (2007) 19.
[13] B. Lorenz, J. Lenzi, J. Cmaidalka, R.L. Meng, Y.Y. Sun, Y.Y. Xue, C.W. Chu, Physica C 383 (2002) 191.
[14] Y. Zhu, W. Zhang, F. Hua, L. Li, J. Alloys Compd. 485 (2009) 439.
[15] K.E. Johansson, T. Palm, P.-E. Werner, J. Phys. E 1 (1980) 1289.
[16] P.E. Werner, L. Eriksson, S. Salome, SCANPI, A Program for Evaluating Guinier Photographs, Stockholm University, Stockholm, 1980.
[17] P.E. Werner, L. Eriksson, M. Westerdahl, J. Appl. Crystallogr. 18 (1985) 367.
[18] P.E. Werner, Ark. Kemi. 31 (1969) 513.
[19] J. Tauc, R. Grigorovici, A. Vancu, Phys. Stat. Sol. 15 (1966) 627.
[20] (a) P.E. Blöchl, Phys. Rev. B 50 (1994) 17953;
(b) G. Kresse, J. Joubert, Phys. Rev. B 59 (1999) 1758.
[21] (a) G. Kresse, J. Hafner, Phys. Rev. B 47 (1993) 558;
(b) G. Kresse, J. Furthmüller, Phys. Rev. B 54 (1996) 11169.
[22] J.P. Perdew, Y. Wang, Phys. Rev. B 45 (1992) 13244.
[23] H.J. Monkhorst, J.D. Pack, Phys. Rev. B 13 (1972) 5188.
[24] F. Gingl, T. Vogt, E. Akiba, J. Alloys Compd. 306 (2000) 127.
[25] N.N. Roy, Nature 206 (1965) 501.
[26] M. Imai, K. Nishida, T. Kimura, H. Kitazawa, H. Abe, H. Kito, K. Yoshii, Physica C 382 (2002) 361.
[27] S. Kuroiwa, T. Kakiuchi, H. Sagayama, H. Sawa, J. Akimitsu, Physica C 460–462 (2007) 154.
[28] K.R. Andress, E. Alberti, Z. Metallkd. 27 (1935) 126.